OC6 Phase Ia Definition Document: Validation of Nonlinear Hydrodynamic Loading on the DeepCwind Semisubmersible

Amy Robertson, Philipp Mucha, Fabian Wendt, and Jason Jonkman

National Renewable Energy Laboratory

NREL is a national laboratory of the U.S. Department of Energy
Office of Energy Efficiency & Renewable Energy
Operated by the Alliance for Sustainable Energy, LLC

This report is available at no cost from the National Renewable Energy Laboratory (NREL) at www.nrel.gov/publications.

Contract No. DE-AC36-08GO28308

Technical Report
NREL/TP-5000-80803
February 2022

OC6 Phase Ia Definition Document: Validation of Nonlinear Hydrodynamic Loading on the DeepCwind Semisubmersible

Amy Robertson, Philipp Mucha, Fabian Wendt, and Jason Jonkman

National Renewable Energy Laboratory

Suggested Citation
Robertson, Amy, Philipp Mucha, Fabian Wendt, Jason Jonkman. 2022. *OC6 Phase Ia Definition Document: Validation of Nonlinear Hydrodynamic Loading on the DeepCwind Semisubmersible*. Golden, CO: National Renewable Energy Laboratory. NREL/TP-5000-80803. https://www.nrel.gov/docs/fy22osti/80803.pdf

NREL is a national laboratory of the U.S. Department of Energy
Office of Energy Efficiency & Renewable Energy
Operated by the Alliance for Sustainable Energy, LLC

This report is available at no cost from the National Renewable Energy Laboratory (NREL) at www.nrel.gov/publications.

Contract No. DE-AC36-08GO28308

Technical Report
NREL/TP-5000-80803
February 2022

National Renewable Energy Laboratory
15013 Denver West Parkway
Golden, CO 80401
303-275-3000 • www.nrel.gov

NOTICE

This work was authored by the National Renewable Energy Laboratory, operated by Alliance for Sustainable Energy, LLC, for the U.S. Department of Energy (DOE) under Contract No. DE-AC36-08GO28308. Funding provided by the U.S. Department of Energy Office of Energy Efficiency and Renewable Energy Wind Energy Technologies Office. The views expressed herein do not necessarily represent the views of the DOE or the U.S. Government.

Cover Photos by Dennis Schroeder: (clockwise, left to right) NREL 51934, NREL 45897, NREL 42160, NREL 45891, NREL 48097, NREL 46526.

Acknowledgments

The authors would like to acknowledge the support of the MaRINET2 project (European Union's Horizon 2020 grant agreement 731084), which supplied the tank test time and travel support to accomplish the experimental campaign. The support of Maritime Research Institute Netherlands (MARIN) in the preparation, execution of the model tests, and evaluation of the uncertainties was essential for this study. MARIN's contribution was partly funded by the Dutch Ministry of Economic Affairs through Tyrosine Kinase Inhibitors - Amsterdam Reproduction & Development funding programs. We would additionally like to thank the Norwegian University of Science and Technology for their support throughout the Offshore Code Comparison Collaboration, Continued, with Correlation, and unCertainty (OC6) Phase Ia project.

Executive Summary

The purpose of this paper was to provide participants of the Offshore Code Comparison Collaboration, Continued, with Correlation, and unCertainty (OC6) project, run under the International Energy Agency Wind Task 30, the information required to build and simulate models of the OC5-DeepCwind offshore floating wind system. The goal of OC6 Phase Ia was to validate these simulation models against measurements from wave-tank testing of the system under a variety of wave conditions, with a focus on the low-frequency hydrodynamic loading. Results from this project can be found in the summary paper (Robertson et al. 2020), and all simulation results, as well as the experimental data, can be found on the website: https://a2e.energy.gov/data/oc6/oc6.phase1a.

Table of Contents

List of Figures

List of Tables

1 Introduction

The OC6 project is focused on validating offshore wind energy modeling tools by comparing simulated responses of select offshore wind systems to physical test data. The four phases (or work packages) of OC6 concentrate on critical phenomena important to estimating offshore wind system loads. OC6 encompasses the development and application of uncertainty quantification and a three-way validation procedure among engineering-level tools, higher-fidelity tools, and measurements.

The objective of OC6 Phase I was to investigate the persistent underprediction (about 20% on average) of the structural loads in the Offshore Code Comparison Collaboration, Continued with Correlation (OC5)-DeepCwind floating semisubmersible wind system, as observed within the previous OC5 Phase II project (Robertson 2017). The OC5 results indicated that much of this underprediction originates from the low-frequency response of the system at the surge/pitch natural frequencies, resulting from nonlinear hydrodynamic loading and/or overprediction of hydrodynamic damping. This work package therefore focused on better understanding the low-frequency response behavior, the applicability of computational fluid dynamics models and engineering-level hydrodynamic models for predicting the nonlinear hydrodynamic loading, and the level of uncertainty in the measured response characteristics.

To address this objective, two experimental campaigns were developed and performed in 2017 and 2018 by a subgroup of the OC5 project:

- **Floating test campaign:** A simplified OC5-DeepCwind semisubmersible model (no turbine, rigid tower) was moored to three taut-spring lines and subjected to motion decay and wave tests (regular and irregular waves), during which motion amplitudes of the model were measured (see Figure 1a). The purpose of this test campaign was to examine the repeatability of the low-frequency response of the system to wave excitation and determine the level of uncertainty in the response behavior.
- **Constrained test campaign:** The same model, but without the tower present, was fixed to a carriage and subjected to towing, forced oscillation, and wave tests (regular and irregular waves), during which forces exerted upon the model were measured (see Figure 1b). The purpose of this test campaign was to examine the hydrodynamic loading contributions by separating the wave excitation and radiation forces.

Both model test campaigns were performed in the Concept Basin of the Maritime Research Institute Netherlands (MARIN) in Wageningen, Netherlands (Gueydon 2018), and the first test was within the framework of the MaRINET2 project (Bachynski 2017).

Both experimental campaigns were examined within Phase Ia of the OC6 project. The purpose of this report is to supply the needed information to participants of the OC6 project to build and simulate the experimental campaigns. Findings from the OC6 Phase Ia project can be found in (Robertson et al. 2020). An additional validation campaign, which focused on the components of this system, was completed in 2021 to further analyze the low-frequency issue and was named OC6 Phase Ib. Information on this project can be found in (Robertson et al. 2021).

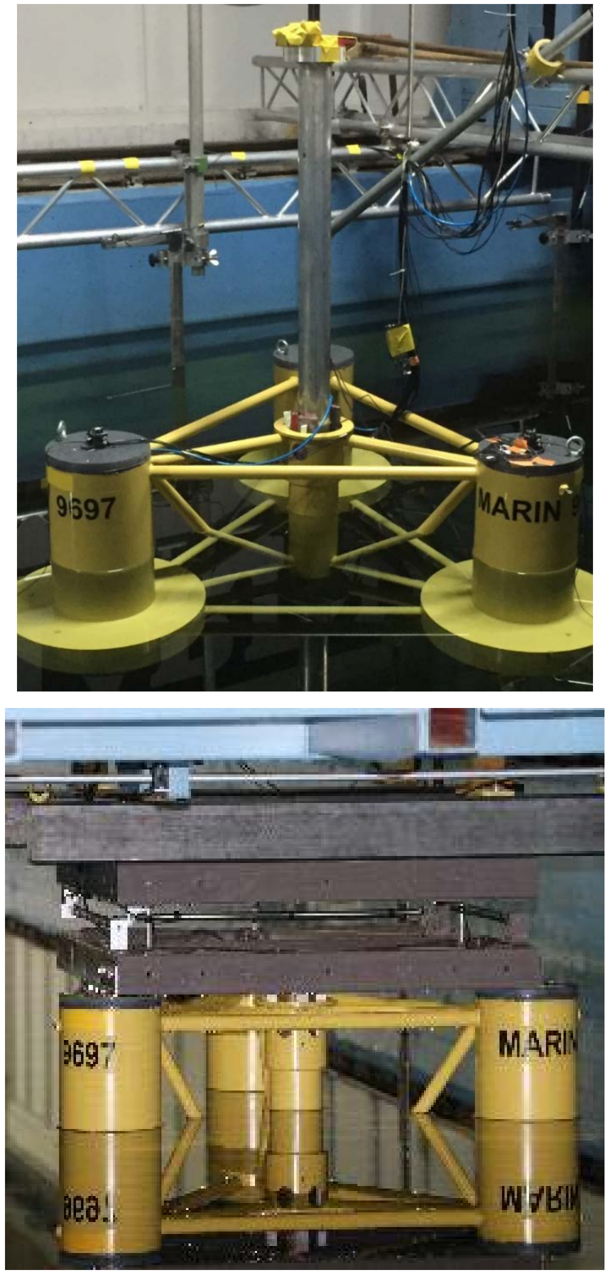

Figure 1. DeepCwind floating semisubmersible experimental campaigns at MARIN Concept Basin (two configurations).

(a) Floating test configuration: semisubmersible with rigid tower. *Photo by Amy Robertson, National Renewable Energy Laboratory (NREL)*

(b) Constrained test configuration: semisubmersible fixed to carriage. *Photo by Amy Robertson, NREL*

2 Experimental Setup

Both experimental campaigns were performed at the MARIN Concept Basin, which has a length of 220 meters (m), a width of 4 m, and a depth of 3.6 m (model scale). The basin is equipped with a stiff overhead carriage that runs over the full length of the basin. The wave generator consists of eight autonomously driven hinged flaps and a wave reflection compensation technology. A passive wave absorber is installed at the downstream end of the basin.

The right-handed coordinate system that was used in this study originates at the center of the main column of the semisubmersible at the still-water line, with positive x being in the direction of propagating waves (head waves equivalent to 0°), and z being up (see Figure 2). All information in this document is presented in full scale (with the exception of the experimental setup), and simulations are also reported at full scale.

2.1 Floating Test Configuration

The model of the floater at scale 1:50 was available from previous experiments. For the floating experimental campaign, the wind turbine was removed, and the tower was changed to a stout, rigid one with inertia properties similar to the properties for the OC5-DeepCwind turbine and tower combined (see Figure 1a). The wetted geometry in the tests was the same as in tests for the OC5 project (Robertson et al. 2020).

The model was tested at a design draught condition of 20 m at full scale. The longitudinal position of the structure in the tank was 40.44 m (model scale) away from the wave generator and in the center of the tank widthwise. A detailed description of the geometry is available from (Robertson et al. 2014). Figure 2 shows the orientation of the model and the locations of wave probes and fairleads. Coordinates of the wave probe positions are given in Figure 2 and Table 1.

The model was moored using three fairleads installed on the edge of the base of each of the three columns, forming the triangle shape of the semisubmersible (see Figure 3). Its measured mass and inertia properties are summarized in Table 2; hydrodynamic properties are summarized in Table 3. Rigid-body motions were measured with an optical system on top of each of the three columns. The tension of the mooring lines was measured as well. The axial stiffness of the spring was 48.9 kilonewton meters (kN/m), and the tension at rest was 1,122.5 kN featuring a pretension angle of 34.5°, as shown in Figure 3 and Table 4. Further mooring properties are provided in Tables 4 and 5.

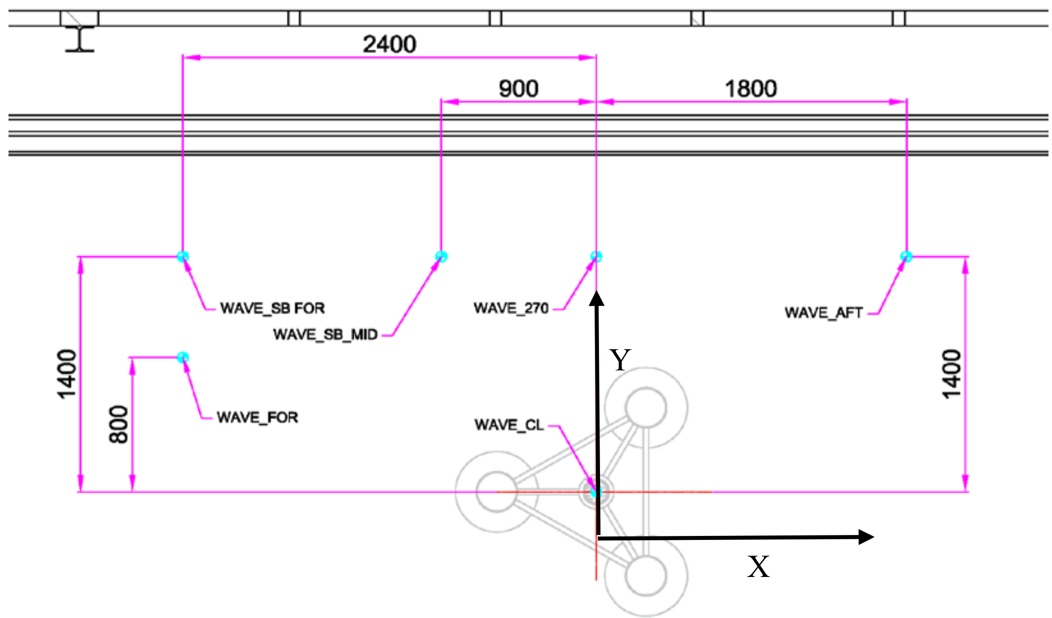

Figure 2. Schematic of the position and orientation of the semisubmersible within the tank, including wave probes and fairleads, and introduction of the coordinate system in the horizontal plane.

Distances shown in model scale (millimeters [mm]).

Table 1. Locations of Wave Probes (full scale; see Figure 2)

Wave Probe	X [m]	Y [m]
WAVE_CL	0	0
WAVE_270	0	70
WAVE_AFT	90	70
WAVE_SB_MID	-45	70
WAVE_SB_FOR	-120	70
WAVE_FOR	-120	40

Table 2. Mass and Inertia Properties of the System for Tests in Moored Condition

Property	Units	Measured
Mass	kg	1.419625E+7
Gravity	m/s^2	9.8124
Longitudinal center of gravity (CG)	m	0
Transverse CG	m	0
Vertical CG relative to still-water line	m	-7.53
Roll radius of gyration with respect to CG	m	30.14
Pitch radius of gyration with respect to CG	m	30.09
Yaw radius of gyration with respect to CG	m	31.61
Ixx with respect to system CG	kg·m^2	1.2898E+10
Iyy with respect to system CG	kg·m^2	1.2851E+10
Izz with respect to system CG	kg·m^2	1.4189E+10

Table 3. Hydrodynamic Properties of the System for Tests in Moored Condition

Property	Units	Value
Water depth	m	180
Water density	kg/m3	1,025
Displaced volume	m3	14,039.8

Table 4. Mooring Line Properties of the System for Tests in Moored Condition

Property	Units	Measured
Line angle	degrees	34.5
EA	N	2.710624E+6
Unstretched line length	m	55.432
Preload	kN	1,122.5
Mooring stiffness	kN/m	48.9

Table 5. Coordinates of Fairleads and Anchors

Fairlead/Anchor	X [m]	Y [m]	Z [m]
Fairlead – Line 1 (FL1)	-40.87	0.0	-14
Fairlead – Line 2 (FL2)	20.43	-35.39	-14
Fairlead – Line 3 (FL3)	20.43	35.39	-14
Anchor – Line 1 (AL1)	-105.47	0.00	-58.4
Anchor – Line 2 (AL2)	52.73	-91.34	-58.4
Anchor – Line 3 (AL3)	52.73	91.34	-58.4

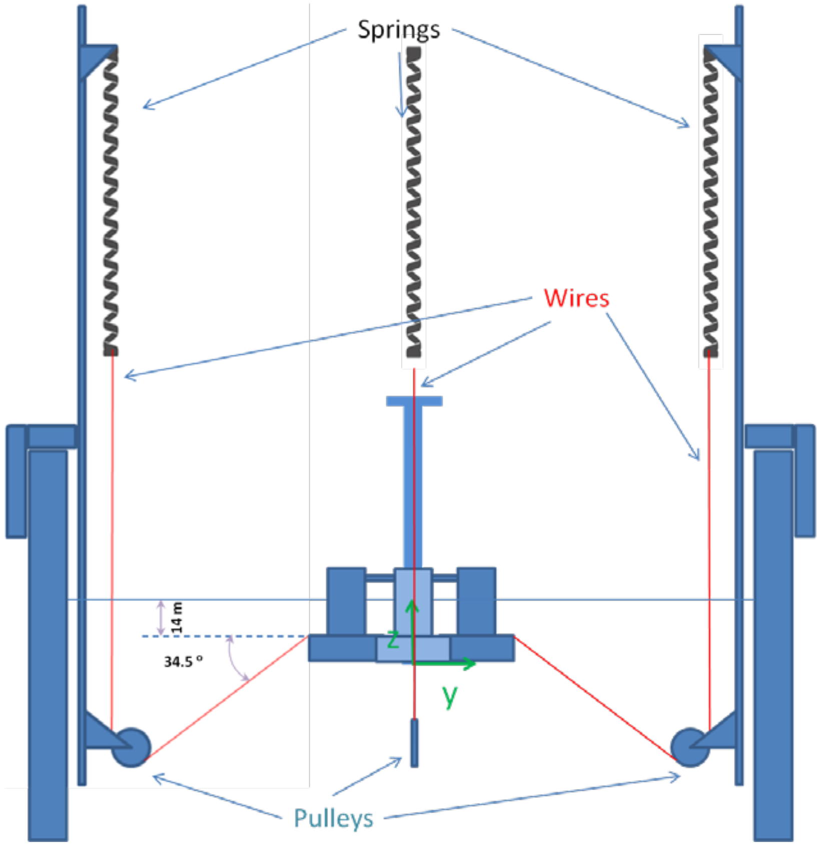

Figure 3. Experimental setup of taut-spring lines

2.2 Constrained Test Configuration

The constrained configuration uses the same floater as for the moored test campaign, but the tower is removed so that it can now attach to the fixation frame of the carriage (see Figure 4). This configuration allows for the system to be held fixed under wave loading and to measure the total hydrodynamic force. It also allows for forced motion of the floater in the surge direction. The middle of the frame is offset from the semisubmersible at (-5.5, 0.0, 39.5 m) relative to the floater reference system. For the wave cases, the structure is at the same location in the tank as the neutral position of the moored condition, and the WAVE_FOR wave probe is at the same longitudinal position for both configurations. Only two wave probes are present for the constrained tests, and their locations are provided in Figure 5 and Table 6.

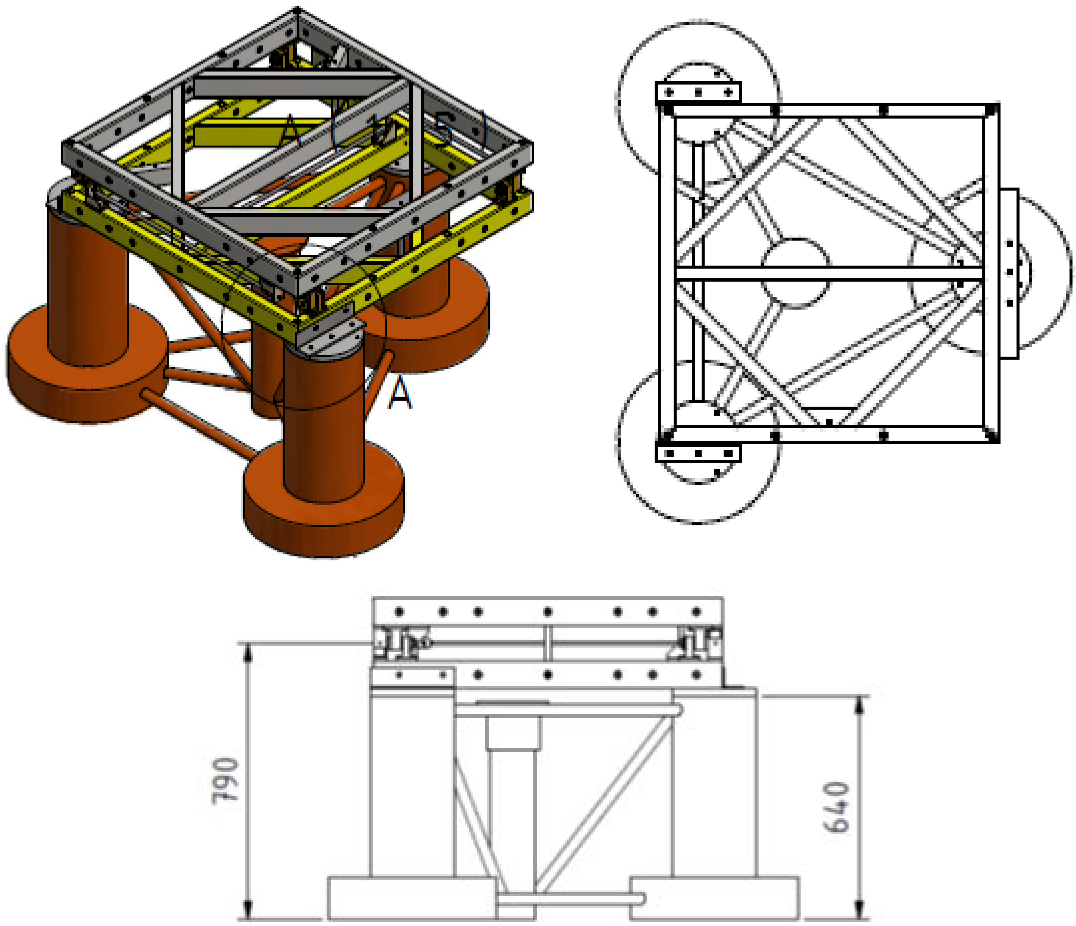

Figure 4. Computer-aided design drawings of the carriage frame used for captive model tests illustrating the fixation of the model to the six-component frame

Distances are in model scale [mm].

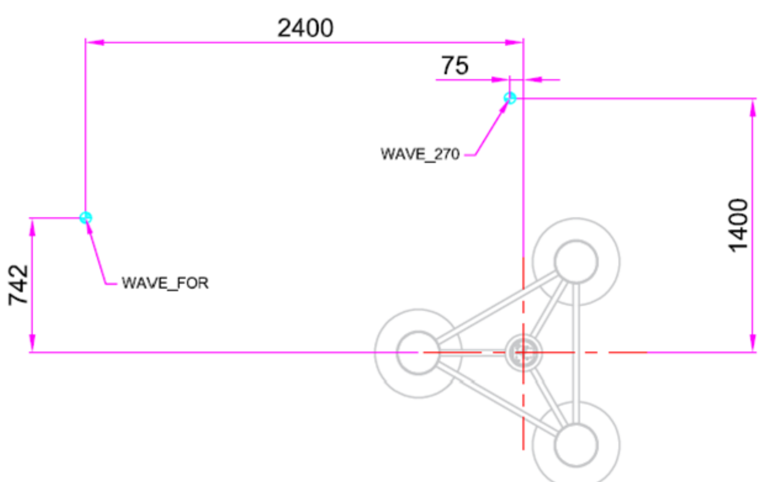

Figure 5. Location of wave probes for fixed-test configuration.

Distances are in model scale [mm].

Forces/moments on the model were measured using a six-component gauge installed with the fixation frame. Table 7 provides the mass and inertia properties for the model, including ballasting and the bottom half of the carriage frame, measurement equipment, and cables, which are required for reduction of measurement data. In addition, the speed and acceleration of the carriage were measured, as was the acceleration of the floater.

Table 6. Locations of Wave Probes (see Figure 5)

Wave Probe	X [m]	Y[m]
WAVE_270	-3.75	70
WAVE_FOR	-120	37.1

Table 7. Mass and Inertia Properties of the Model Including Ballasting and the Bottom Half of the Six-Component Frame, Measurement Equipment, and Cables

Property	Unit	As-Built (including frame and equipment)
Mass	kg	1.8074E7
Longitudinal center of gravity (CG) relative to floater reference system	m	0.90
Transverse CG relative to floater reference system	m	0.03
CG relative to still-water line	m	-4.42
Roll radius of gyration with respect to CG	m	26.66
Pitch radius of gyration with respect to CG	m	26.46
Yaw radius of gyration with respect to CG	m	30.62

3 Load Case Description

The load cases simulated for OC6 Phase Ia are summarized in the following sections, along with the associated outputs. Outputs are at full scale in the units provided by the table. The load cases highlighted in yellow are cases used for model calibration work. The remainder of the load cases are used for validation.

3.1 Load Case 1: Towing Tests, Constrained Configuration

Straight-line towing tests in calm water were performed to represent a current-only condition using six different carriage speeds. The model was accelerated from rest until the desired carriage speed was attained. Table 8 provides the details for the associated simulations. A list of simulation outputs to be reported by the participants is given in Table 9. Time-varying results (e.g., from computational fluid dynamics simulations) should be time-averaged over a suitable range toward the end of the time record once the computational quantity of interest has settled around a constant value. Note that for Load Case (LC) 1.x and 2.x, simulation outputs were requested both for the total load measurement and for just the hydrodynamic component (removing inertia). Two different files were uploaded with the extensions .tot and .hyd, representing the total load measurement and just the hydrodynamic component, respectively.

Table 8. LC 1.x: Current-Only Simulations

Load Case	Current Speed (FS)* [m/s]	Current Speed (MS)* [m/s]	Froude #
1.1	0.5	0.0707	0.046
1.2	1.0	0.1414	0.092
1.3	1.5	0.2121	0.138
1.4	2.0	0.2828	0.184
1.5	2.5	0.3535	0.23
1.6	3.0	0.4242	0.28

**FS = full scale, MS = model scale. Froude number based on column diameter of 12 m.*

Table 9. Simulation Outputs of Towing Tests (One output file for all current speeds.

Output Column	Output Description	Unit
1	Towing speed	m/s
2	Hydrodynamic force (x-dir)	N
3	Hydrodynamic moment (about y-axis)	N·m

3.2 Load Case 2: Forced Oscillation Tests, Constrained Configuration

Forced oscillation tests in the surge mode of motion were conducted using different oscillation periods and motion amplitudes. These were chosen in accordance with practically relevant surge velocities, motion periods, and the anticipated maximum feasible acceleration of 0.4 m/s^2 for the carriage. Carriage speed was prescribed and contained a ramping phase at the beginning of the tests. The time series of the surge motion and acceleration were made available for use as an input for motion prescription in the simulations and to determine the inertia component of the force measurement.

Table 10 contains the details of each load case. The provision of time series of specified hydrodynamic forces and moments covering 20 periods of oscillation (*T*), which are unaffected by transient behavior because of motion ramping, and so on, was requested (see Table 11). The force and moment signals should match what would be measured in the tank experiment, which would include both the hydrodynamic loading and inertial loading (from acceleration of the body).

Table 10. LC 2.x: Parameters for Forced Oscillation in Surge Direction

Load Case	Amplitude [m]	Period, *T* [s]	Max. Speed [m/s]	Max. Acceleration [m/s^2]
2.1	40.11	105	2.397	0.143
2.2	30.07	105	1.807	0.109
2.3	9.601	31.19	1.932	0.389
2.4	6.444	31.19	1.306	0.265
2.5	3.367	20.99	1.004	0.299
2.6	4.481	20.99	1.340	0.400

Table 11. Simulation Outputs of Forced Oscillation Tests

Output Column	Output Description	Units	Output Range (first peak after ramping)
1	Time	s	20*T*
2	Forced motion (x-dir)	m	20*T*
3	Force (x-dir)	N	20*T*
4	Moment (about y-axis)	N·m	20*T*

3.3 Load Case 3: Tests in Waves, Constrained Configuration

Tests in regular and irregular waves were performed in both the constrained (LC 3.x) and moored (LC 5.x) conditions. Two regular waves, an irregular wave based on the Joint North Sea Wave Project (JONSWAP) spectrum, and a white noise spectrum were generated. These are similar to the ones investigated within OC5. Waves were calibrated in preparation of the first of the two experimental campaigns, which dealt with the moored model. All generated waves propagate at 0° with respect to the coordinate system in place and will be available for direct implementation in the simulation. Measured waves were provided, and the time range specified in Table 12 is the range of the measured signal that was analyzed and reported on. Simulations should be free of any initial transient effects in this output range. For participants not directly using the measured signal, the regular wave output should be provided starting at zero wave elevation (at the origin), with increasing wave elevation.

Wave height/significant wave heights and period/peak periods are provided in Table 12. These are calculated for the down-selected region of the signal specified in “Simulation Output Range.” If a participant generated their own wave signal, they were encouraged to compare the properties of their signal to the one uploaded to the Confluence site (within the simulation output range), rather than just relying on the specified wave and period properties. Table 13 provides the expected outputs from participants for the LC 3.x simulations.

Table 12. LC 3.x: Parameters for Tests in Waves in Constrained Condition

Load Case	Type	Spectrum	Wave Height/ Significant Wave Height [m]	Period or Peak Period seconds (s)	Total Output Time [s]	Simulation Output Range
3.1	Regular	-	7.0	12.0	600	700.3–1,300.3 s (pts: 7,005–13,004)
3.2	Regular	-	3.95	9.0	600	1,051.7–1,651.7 (pts: 10,518–16,518)
3.3	Irregular	JONSWAP, γ = 3.3	7.4	12.0	10,800 (3 h)	1,946.7–12,746.7 s (pts: 19,467–127,467)
3.4	Irregular	White noise	6.7	6–26	10,800 (3 h)	1,935.7–12,735.7 s (pts: 19,357–127,357)

A preliminary analysis of the wave spectrum for LC 3.3 showed some level of discrepancy between the JONSWAP spectrum generated with the parameters given in Table 12, and the spectrum calculated from the measured wave. These findings are illustrated in Figure 6. Additional analysis regarding the definition of the correct wave spectrum is encouraged if the measured wave elevation signal cannot be prescribed directly.

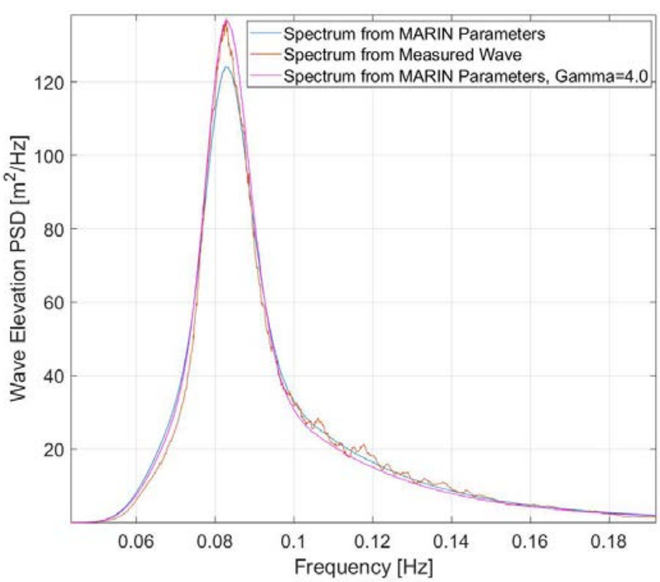

Figure 6. Comparison of the irregular wave spectrum (Load Case 3.3) derived from the measured wave and the theoretical JONSWAP spectrum defined through the parameters given in Table 12

Table 13. Simulation Outputs of Tests in Waves in Constrained Condition for Each Load Case 3.x of Table 11

Output Column	Output Description	Units
1	Time	s
2	Wave elevation	m
3	Hydrodynamic force (x-dir)	N
4	Hydrodynamic force (y-dir)	N
5	Hydrodynamic force (z-dir)	N
6	Hydrodynamic moment (about x-axis)	N·m
7	Hydrodynamic moment (about y-axis)	N·m
8	Hydrodynamic moment (about z-axis)	N·m
9	Force (x-dir) on upstream column (upper column)	N
10	Force (x-dir) on upstream column (base column)	N
11	Force (x-dir) on starboard column (upper column)	N
12	Force (x-dir) on starboard column (base column)	N
13	Force (x-dir) on main column	N
14	Mean value for columns 3–13 (11 rows)	N/N·m

3.4 Load Case 4: Free Decay, Floating Configuration

Motion decay tests were conducted in the moored setup in surge, heave, roll, and pitch modes of motion. The tests were performed by pushing on the structure from a nearby carriage. Table 14 reflects the test matrix of experiments to be simulated. Requested outputs are specified in Table 15. The appendix describes the procedure to compute damping characteristics based on the *pq*-method (Helder et al. 2013). Participants supplied the time-domain results of the free decay, and the National Renewable Energy Laboratory calculated the frequencies/damping. The simulation output was 1,000 s, with the standard 0.1 s time step.

Table 14. LC 4.x: Parameters for Free-Decay Tests

Load Case	Mode	Offset From Equilibrium Position/Orientation	Total Simulation Time
4.1	Surge	-1.86 m	1,000 s
4.2	Surge	-3.39 m	1,000 s
4.3	Heave	-1.06 m	1,000 s
4.4	Heave	-1.57 m	1,000 s
4.5	Pitch	-2.21°	1,000 s
4.6	Pitch	-3.95°	1,000 s

Table 15. Outputs for Free-Decay Tests for Each Load Case 4.x of Table 14

Output Column	Output Description	Units
1	Time	s
2	Motion amplitude (x-dir)	m
3	Motion amplitude (y-dir)	m
4	Motion amplitude (z-dir)	m
5	Motion amplitude (about x-axis)	deg
6	Motion amplitude (about y-axis)	deg
7	Motion amplitude (about z-axis)	deg

3.5 Load Case 5: Tests in Waves, Floating Configuration

The same waves and output time range from Load Case 3.x were used for the floating configuration, Load Case 5.x (as shown in Table 16), but different outputs were requested for this configuration. These are described in Table 17.

Table 16. LC 5.x: Parameters for Tests in Waves in Moored Condition

Load Case	Type	Spectrum	Wave Height/ Significant Wave Height [m]	Period or Peak Period [s]	Total Output Time [s]	Output Range [s]
5.1	Regular	-	7.0	12.0	600	700.3–1,300.3 (pts: 7,005–13,004)
5.2	Regular	-	3.95	9.0	600	1,051.7–1,651.7 (pts: 10,518–16,518)
5.3	Irregular	JONSWAP, $\gamma = 3.3$	7.4	12.0	10,800 (3 h)	1,946.7–12,746.7 (pts: 19,467–127,467)
5.4	Irregular	White noise	6.7	6–26	10,800 (3 h)	1,935.7–12,735.7 (pts: 19,357–127,357)

Table 17. Simulation Outputs for Tests in Waves in Moored Condition for Each Load Case 5.x of Table 16

Output Column	Output Description	Units
1	Time	s
2	Wave elevation	m
3	Motion amplitude (x-dir) – surge	m
4	Motion amplitude (y-dir) – sway	m
5	Motion amplitude (z-dir) – heave	m
6	Motion amplitude (about x-axis) – roll	deg
7	Motion amplitude (about y-axis) – pitch	deg
8	Motion amplitude (about z-axis) – yaw	deg
9	Mooring tension – FL1	N
10	Mooring tension – FL2	N
11	Mooring tension – FL3	N

4 Uncertainty Assessment

Quantifying the uncertainty in experimental results is a critical step in properly validating numerical simulation tools for designing floating wind turbines; without a good understanding of the experimental uncertainties, it is impossible to determine if numerical simulation tools can capture the physics with acceptable accuracy. A detailed description of the process used to calculate uncertainty in the floating campaign is provided by (Robertson et al. 2018, 2019).

5 Data Availability and Format

The measurements from these two experimental campaigns, as well as the simulation results from participants in the OC6 project, are available for download on the Data Archive and Portal at https://a2e.energy.gov/data/oc6/oc6.phase1a. The naming of the data files follows the convention oc6.phase1a.name.loadcase.txt. The experimental measurements use the name "EXP0"; participants use a four-letter acronym.

Most data files end in .txt., but for Load Cases 1 and 2, the files have the extensions .tot and .hyd, representing the total load measurement and just the hydrodynamic component, respectively. Results are provided for all simulations cases detailed in this report. Further details on the results from the OC6 Phase Ia project can be found in the project summary (Robertson et al. 2020).

References

Bachynski, E. 2017. *Follow-on Testing of the OC5 Semisubmersible to Address Hydrodynamic Modelling Uncertainties*. MARINET-TA1-OC5-1088.

Gueydon, S. and R. Van Alfen. 2018. *MARINET 2 OC6 Model Tests: A series of tests focusing on the hydrodynamics of the OC5 Semisubmersible.* Report No. 29305-01, v. 2.3

Helder, J.A. and M. Pietersma. 2013. *UMaine – DeepCwind/OC4 Semi Floating Wind Turbine Repeat Tests*. MARIN Report No. 27005-1-OB.

Robertson, A, J. Jonkman, M. Masciola, H. Song, A. Goupee, A. Coulling, C. Luan. 2014. *Definition of the Semisubmersible Floating System for Phase II of OC4.* 43 pp.; Golden, CO: National Renewable Energy Laboratory. NREL/TP-5000-60601.

Robertson, A. et al. 2017. "OC5 Project Phase II: Validation of Global Loads of the DeepCwind Floating Semisubmersible Wind Turbine." *Energy Procedia*, Vol. 137.: pp 38–-57.

Robertson, AN, EE Bachynski, S Gueydon, F Wendt, P Schünemann, & J. Jonkman. 2018. "Assessment of Experimental Uncertainty for a Floating Wind Semisubmersible Under Hydrodynamic Loading." *Proceedings of the ASME 2018 37th International Conference on Ocean, Offshore and Arctic Engineering. Volume 10: Ocean Renewable Energy*. Madrid, Spain. June 17–22, 2018. V010T09A076. ASME. https://doi.org/10.1115/OMAE2018-77703.

Robertson, A., E. Bachynski, S. Gueydon, F. Wendt, P. Schünemann. 2019. "Total Experimental Uncertainty in Hydrodynamic Testing of a Semisubmersible Wind Turbine, Considering Numerical Propagation of Systematic Uncertainty." *Ocean Engineering* 195: 106605.

Robertson, A. N., et al. 2020. "OC6 Phase I: Investigating the underprediction of low-frequency hydrodynamic loads and responses of a floating wind turbine." *Journal of Physics: Conference Series* 1618: 032033.

Robertson, Amy, and Lu Wang. 2021. "OC6 Phase Ib: Floating Wind Component Experiment for Difference-Frequency Hydrodynamic Load Validation" *Energies* 14, no. 19: 6417. https://doi.org/10.3390/en14196417

Appendix. Damping Coefficient Methodology

The parameter identification procedure proposed by Helder et al. (2013) is recommended for the analysis of free-decay motion. Figure A-1 shows a typical time history of a lightly damped system undergoing motion decay from an initial offset. The underlying mathematical model is a classic mass-damper-spring system for a free extinction test, including linear and quadratic damping

$$a_{\phi\phi}\ddot{\phi} + b^1_{\phi\phi}\dot{\phi} + b^2_{\phi\phi}\dot{\phi}|\dot{\phi}| + c_{\phi\phi}\phi = 0$$

where

ϕ = a generalized degree of freedom

$a_{\phi\phi}$ = Total mass (physical + hydrodynamic) [kg] for translational modes of motion, total moment of inertia (physical + hydrodynamic) [kg·m^2] for rotational modes of motion

$b^1_{\phi\phi}$ = Linear damping coefficient [N·s/m] for translational modes of motion, [N·m·s/rad] for rotational modes of motion

$b^2_{\phi\phi}$ = Quadratic damping coefficient [N·s^2/m^2] for translational modes of motion, [N·m·s^2/rad^2] for rotational modes of motion

$c_{\phi\phi}$ = Restoring coefficient [N/m] for translational modes of motion, [N·m/rad] for rotational modes of motion

T_ϕ = Natural period of motion [s].

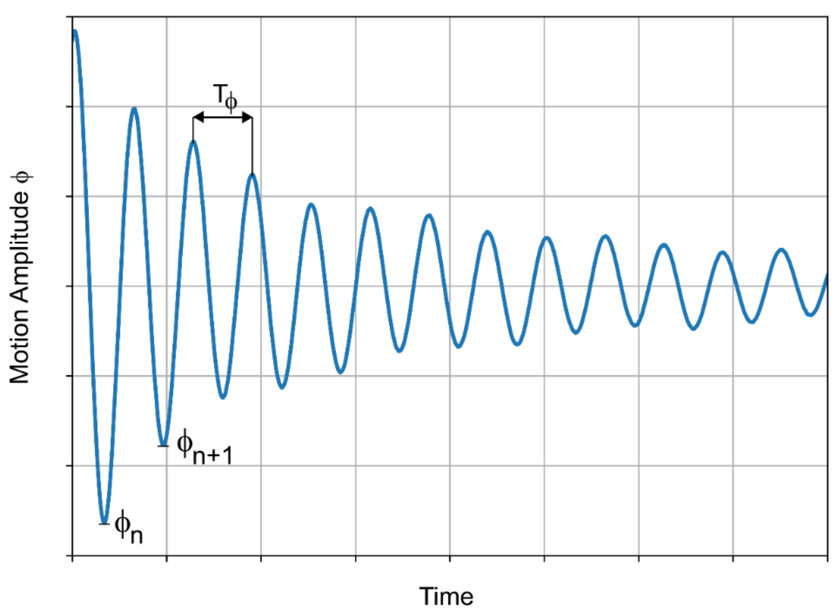

Figure A-1. Schematic of a typical free-decay motion time series and relevant metrics

The procedure is based on linear regression analysis of the decrease in normalized motion amplitudes with respect to the mean motion amplitude as shown in Figure A-2. For the present investigation, parameters p, y-intercept, and q, slope of the linear fit, are used as metrics for comparison. They are directly proportional to the linear and quadratic damping of the signal.

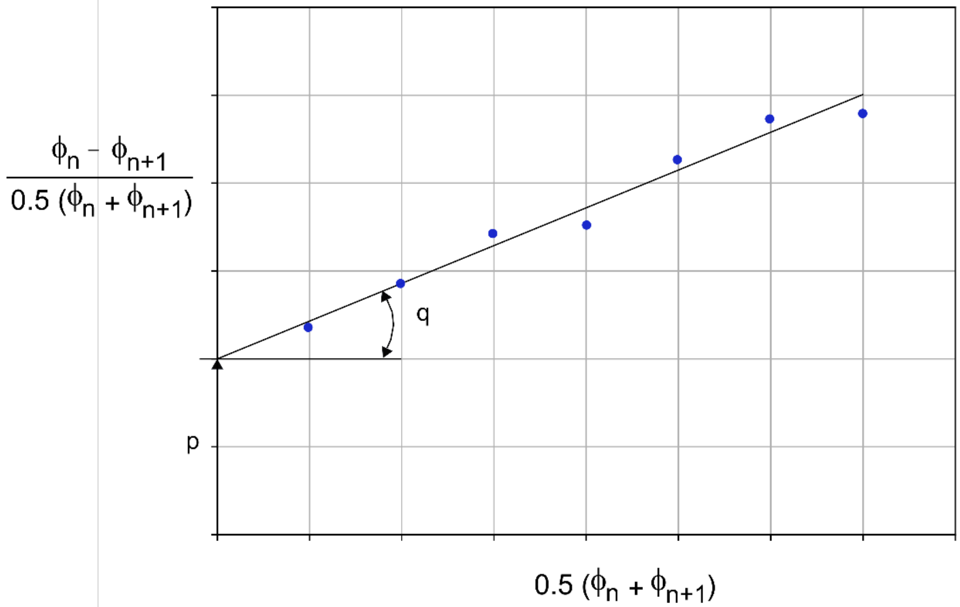

Figure A-2. Schematic of regression analysis of normalized motion amplitude decrease from decay tests